

Accepted Manuscript

Exact closed-form solutions of a fully nonlinear asymptotic two-fluid model

Alexei F. Cheviakov

PII: S0167-2789(16)30418-3
DOI: <https://doi.org/10.1016/j.physd.2018.01.001>
Reference: PHYSD 31995

To appear in: *Physica D*

Received date: 17 August 2016
Accepted date: 3 January 2018

Please cite this article as: A.F. Cheviakov, Exact closed-form solutions of a fully nonlinear asymptotic two-fluid model, *Physica D* (2018), <https://doi.org/10.1016/j.physd.2018.01.001>

This is a PDF file of an unedited manuscript that has been accepted for publication. As a service to our customers we are providing this early version of the manuscript. The manuscript will undergo copyediting, typesetting, and review of the resulting proof before it is published in its final form. Please note that during the production process errors may be discovered which could affect the content, and all legal disclaimers that apply to the journal pertain.



Exact Closed-Form Solutions of a Fully Nonlinear Asymptotic Two-Fluid Model

Alexei F. Cheviakov^a

Department of Mathematics and Statistics, University of Saskatchewan, Canada.

January 14, 2018

Abstract

A fully nonlinear model of Choi and Camassa [1] describing one-dimensional incompressible dynamics of two non-mixing fluids in a horizontal channel, under a shallow water approximation, is considered. An equivalence transformation is presented, leading to a special dimensionless form of the system, involving a single dimensionless constant physical parameter, as opposed to five parameters present in the original model. A first-order dimensionless ordinary differential equation describing traveling wave solutions is analyzed. Several multi-parameter families of physically meaningful exact closed-form solutions of the two-fluid model are derived, corresponding to periodic, solitary, and kink-type bidirectional traveling waves; specific examples are given, and properties of the exact solutions are analyzed.

1 Introduction

Over the years, in order to describe specific physical settings, such as, for example, surface and internal waves, multiple simplified models of the systems of Euler and Navier-Stokes fluid dynamics equations have been derived, aiming at the reduction of the mathematical complexity of the full set of equations, while retaining essential properties of phenomena of interest and providing sufficient physical insight and computational precision. Basic examples of such simplifications include dimension reductions, linearizations, and more general approximations involving asymptotic relationships. Fundamental nonlinear partial differential equations (PDEs) of mathematical physics, such as Burgers', Korteweg-de Vries (KdV), nonlinear Schrödinger, and Kadomtsev-Petviashvili (KP) equations, as well as many other important models like shallow water equations, Camassa-Holm and Degasperis-Procesi (DP) equations, arise in the context of fluid dynamics. Importantly, such reduced models were often found to exhibit rich mathematical structure, such as integrability, Hamiltonian structure, existence of infinite hierarchies of conservation laws, and solutions in the form of single and/or multiple nonlinear solitary waves (solitons, peakons, etc.). In many cases, exact solutions of reduced models correspond to, and in fact closely describe, physical phenomena. Examples are provided by solitary wave solutions of the KdV equation modeling long waves in shallow channels, periodic solutions of the KP equa-

^aAlternative English spelling: Alexey Shevyakov. Electronic mail: shevyakov@math.usask.ca

tion modeling crossing swell-type shallow water surface waves, and internal waves. Classical nonlinear wave models are reviewed, for example, in [2–5].

In the present work, we consider a model of nonlinear internal waves in a stratified system of two non-mixing fluids of different densities in a long horizontal channel within the gravity field. This two-fluid model has been derived in [1] (see also [6, 7]) through layer-averaging, under an asymptotic “shallow water” assumption of a small ratio of the fluid channel depth to the characteristic wavelength, yet without assuming that wave amplitudes are small compared to the fluid layer depths. The model is one-dimensional, involving four dependent variables (fluid interface displacement, pressure at the interface, and layer-average horizontal velocities) that are functions of time and the spatial coordinate along the channel. The two-fluid equations generalize the weakly nonlinear model of Choi *et al* [8]; they can also be viewed as a two-layer version of the classical Green-Naghdi model [9, 10]. Further extensions have recently appeared in the literature, including a ‘regularized’ two-fluid model [11], a multi-layer model [12], and a rough bottom model [13]. Questions related to the stability of the model at hand and related models, in particular, the Kelvin-Helmholtz instability, are discussed in [11, 14, 15].

The original works [1, 6] dedicated to the two-fluid model at hand study the traveling wave solution ansatz, leading to a curious nonlinear autonomous first-order ordinary differential equation (ODE) for the surface elevation, solved in terms of the squared first derivative, and having a rational-polynomial right-hand side. This ODE is not equivalent to any one of the classical autonomous first-order equations, and is different from ODEs that normally appear in similar contexts in the literature, such as those with the cubic right-hand side, arising, for example, in classical fluid models such as KdV or Su-Gardner equations (e.g., [16]). Implicit solutions of the indicated ODE can be immediately written in terms of integrals, which was done in [6]. In [1], the reduced traveling wave ODE has been shown to admit, for specific parameter relationships, kink- and solitary wave-type traveling wave solutions, which were constructed numerically. In [17], periodic traveling wave solutions were obtained as numerical solutions of the same reduced ODE. No exact closed-form solutions of the two-fluid model have been reported to date.

The main goal of the current contribution is the derivation of exact closed-form solutions of the two-fluid model, representing non-harmonic periodic traveling wave displacements of the fluid interface, traveling solitary waves of depression and elevation, and kink and anti-kink traveling waves. The paper is organized as follows.

In Section 2, the two-fluid equations are reviewed, together with important aspects of their derivation, properties, and related models. Equivalence transformations are used to recast the four equations, for any set of physical and channel parameters, in a general dimensionless form, which involves only a single dimensionless parameter, namely, the fluid density ratio.

The dimensionless form of the two-fluid model, the traveling wave ansatz, and systematically computed integrating factors are used in Section 3 to derive a dimensionless first-order nonlinear ordinary differential equation governing all traveling wave-type solutions of the model, without restrictions on the boundary conditions. The ODE describes the fluid interface elevation for a more general class of solutions than those considered in [1], due to the lack of restrictions on the infinity values of the average fluid velocities. The average velocity values and the pressure at the interface are given by explicit formulas in terms of the fluid interface elevation. As a consequence of the Galilei invariance of the model, the governing ODE is independent of the traveling wave speed.

In Sections 4 and 5, the reduced ODE is utilized to derive new families of exact closed-form solutions of the full two-fluid PDE system. Unlike any previously reported solutions for the considered model, the presented solutions are given by explicit formulae, and include two families of periodic non-harmonic traveling wave solutions, involving elliptic functions. In the first solution family, the fluid interface elevation is expressed in terms of squared elliptic cosine of the traveling wave coordinate, in a way similar to the well-known exact solutions for surface waves (e.g., [2, 16]). The second family of the presented solutions is given by a rational expression involving elliptic functions, and has not previously appeared in the literature in any related context. Further, in the long-wave limit, the aforementioned solutions lead to families of exact expressions describing solitary wave and kink/anti-kink (front-type) solutions of the two-fluid model. Relationships between the solution parameters are investigated, and several examples are considered in detail.

The paper is concluded with Section 7 offering a discussion of properties of the obtained solutions in the context of the existing literature, and outlining related research directions.

The integrating factors and first integrals derived in Section 3 were computed using GeM software package [18, 19] through the direct conservation law construction method [20, 21].

2 The Two-Fluid Model, its Properties, and the Dimensionless Form

2.1 The Governing Equations

The three-dimensional Euler equations of incompressible inviscid fluid flow of constant density ρ in the gravity field are given by

$$\mathbf{v}_t + (\mathbf{v} \cdot \nabla)\mathbf{v} = -\frac{1}{\rho} \text{grad } p - \mathbf{g}, \quad \text{div } \mathbf{v} = 0, \quad (2.1)$$

where $\mathbf{g} = -g\mathbf{k}$ is the gravitational acceleration, $\mathbf{v} = (u(t, \mathbf{x}), v(t, \mathbf{x}), w(t, \mathbf{x}))$ is the velocity vector, and $p(t, \mathbf{x})$ is the fluid pressure. Following Miyata [6], in [1], Choi and Camassa derived a nonlinear (1+1)-dimensional two-fluid model for an approximate asymptotic description of long waves at the fluid interface. We briefly overview the relevant notation and elements of the derivation of the two-fluid equations. Consider an irrotational flow within two fluid layers of depths h_1, h_2 and constant densities ρ_1, ρ_2 (Figure 1). The condition $\rho_1 < \rho_2$ is assumed for a stable stratification.

The incompressible two-dimensional Euler equations in Cartesian coordinates in the (x, z) -plane are given by

$$\begin{aligned} u_x + w_z &= 0, \\ u_t + uu_x + ww_z &= -p_x/\rho, \\ w_t + ww_x + ww_z &= -p_z/\rho - g, \end{aligned} \quad (2.2)$$

with the fluid velocity $\mathbf{u} = u(t, x, z)\mathbf{i} + w(t, x, z)\mathbf{k}$. For the two-fluid model, the PDEs (2.2) are written for both fluid layers. Denote the flow parameters by $(u, w, p) = (u_i, w_i, p_i)$, $i = 1, 2$ for the upper and the lower fluid, respectively. For the two-fluid setup, $z \in [-h_2, h_1]$. In the case of

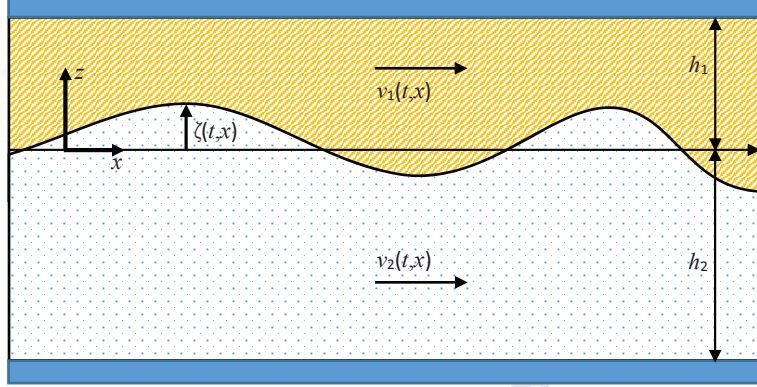


Figure 1: The two-fluid model.

the static equilibrium situation, $0 \leq z \leq h_1$ corresponds to the first fluid layer, and $-h_2 \leq z \leq 0$ to the second one. No-leak boundary conditions are prescribed at the top and bottom horizontal walls of the channel:

$$w_1(t, x, h_1) = w_2(t, x, -h_2) = 0. \quad (2.3)$$

Let $\zeta(t, x)$ denote the vertical displacement of the interface between the fluids. The boundary conditions at the interface $z = \zeta(t, x)$ of the two fluids are the continuity of normal velocity and pressure:

$$\zeta_t + u_1 \zeta_x = w_1, \quad \zeta_t + u_2 \zeta_x = w_2, \quad p_1 = p_2. \quad (2.4)$$

In order to derive the model of interest, an assumption was made that the fluid depth be much smaller than the characteristic length L :

$$h_i/L = \epsilon \ll 1. \quad (2.5)$$

The continuity equation in (2.2) yields

$$w_i/u_i = O(h_i/L) = O(\epsilon) \ll 1.$$

For finite-amplitude waves, it is assumed that

$$u_i/U_0 = O(\zeta/h_i) = O(1), \quad (2.6)$$

where $U_0 = (gH)^{1/2}$, $H = h_1 + h_2$, is the characteristic speed of the problem.

Denote the actual thicknesses of the fluid layers by

$$\eta_1 = h_1 - \zeta, \quad \eta_2 = h_2 + \zeta. \quad (2.7)$$

As shown in [1], the asymptotic computation for the Euler system (2.2) with (2.4) leads to a (1+1)-dimensional PDE system for the unknown interface displacement $\zeta(t, x)$, the hydrostatic

pressure at the interface $P(t, x)$, and the layer-average (depth-mean) horizontal velocities $v_1(t, x)$, $v_2(t, x)$ of the two fluids defined as

$$v_1 = \frac{1}{\eta_1} \int_{\zeta}^{h_1} u_1(t, x, z) dz, \quad v_2 = \frac{1}{\eta_2} \int_{-h_2}^{\zeta} u_2(t, x, z) dz. \quad (2.8)$$

(We note that in [1] and related papers, for the depth-mean velocities, the notation \bar{u}_i was used instead.) Finally, the equations, which we refer to as *the two-fluid model*, are given by

$$\eta_{it} + (\eta_i v_i)_x = 0, \quad (2.9a)$$

$$v_{it} + v_i v_{ix} + g \zeta_x = -\frac{P_x}{\rho_i} + \frac{1}{3\eta_i} (\eta_i^3 G_i)_x + O(\epsilon^4), \quad (2.9b)$$

$$G_i \equiv v_{itx} + v_i v_{ixx} - (v_{ix})^2,$$

$$i = 1, 2.$$

The first-order PDEs (2.9a) are exact; for the purposes of current work, the two remaining PDEs (2.9b) will also be treated as exact, and the $O(\epsilon^4)$ terms will be omitted.

2.2 Discussion of the two-fluid model (2.9)

1) Generalizations and related models. The two-fluid equations (2.9) were derived under the scaling assumption (2.5), not assuming, for example, that the wave amplitudes are small compared to the channel depth. If the latter assumption is imposed, the PDEs (2.9) lead to the Boussinesq approximation, and further, the KdV equation for the case of unidirectional waves [1].

The two-fluid equations (2.9) can be viewed as the two-layer version of the Green-Naghdi homogeneous layer equations [10] (see also [22]), or an extension the weakly nonlinear model of [8]. The PDEs (2.9) were further generalized in [12] where a closed channel with $N \geq 2$ fluid layers was considered. A ‘regularized’ version of the two-fluid model where instead of layer-mean horizontal velocities, velocity values at constant z have been used, has been suggested in [11]. A modification of the two-fluid system to account for an uneven bottom topography has been suggested in [13]. The stability of solutions of the two-fluid model (2.9) and its extensions are discussed, for example, in [1, 23], and references therein.

2) Asymptotic horizontal velocity estimates. The velocity components of a solution of the two-fluid equations are the layer-averaged velocity values (2.8). Approximate values of actual velocities at a fixed value of z can be readily derived. For irrotational flows, the horizontal velocity components can be written as [2]

$$u_i(t, x, z) = u_i^{(0)} - \frac{1}{2}(z \mp h_i)^2 u_{ixx}^{(0)} + O(\epsilon^4), \quad i = 1, 2, \quad (2.10)$$

where $u_1^{(0)}(t, x)$, $u_2^{(0)}(t, x)$ are the horizontal velocity values at the top and bottom channel boundaries $z = h_1$, $z = -h_2$, respectively, and the second term is $O(\epsilon^2)$ [1, 11]. Further, as pointed out in [11], the layer-averaged velocities can be computed from (2.8), (2.10) to yield

$$v_i = u_i^{(0)} - \frac{1}{6} \eta_i^2 u_{ixx}^{(0)} + O(\epsilon^4). \quad (2.11)$$

It is straightforward to show that to the same precision, a backward relationship holds (cf. [2]):

$$u_i^{(0)} = v_i + \frac{1}{6}\eta_i^2 v_{i,xx} + O(\epsilon^4). \quad (2.12)$$

One consequently has an asymptotic expression

$$u_i(t, x, z) = v_i + \left(\frac{1}{6}\eta_i^2 - \frac{1}{2}(z \mp h_i)^2\right) v_{i,xx} + O(\epsilon^4) \quad (2.13)$$

for the horizontal velocities $u_i(t, x, z)$ within the channel in terms of the mean velocity of the corresponding fluid layer.

3) *Boundary conditions in an infinite channel.* A physically natural initial value problem for the two-fluid system (2.9) would be, for example, one stated for $x \in \mathbb{R}$, with appropriate initial conditions, and boundary conditions at infinity:

$$\begin{aligned} v_1(t, x) &\rightarrow V_1^-, & v_2(t, x) &\rightarrow V_2^-, & \zeta(t, x) &\rightarrow \zeta^- & \text{as } x &\rightarrow -\infty, \\ v_1(t, x) &\rightarrow V_1^+, & v_2(t, x) &\rightarrow V_2^+, & \zeta(t, x) &\rightarrow \zeta^+ & \text{as } x &\rightarrow +\infty. \end{aligned} \quad (2.14)$$

For a kink-type solution, for example, one would have $\zeta^- \neq \zeta^+$, whereas for a solitary traveling wave or a multi-soliton situation, $\zeta^- = \zeta^+$. Alternatively, for example, for the case of periodic traveling wave solutions considered below, it may be appropriate to consider PDEs (2.9) in a finite interval $I \subset \mathbb{R}$ with periodic boundary conditions.

As noted in [1], the exclusion of ζ_t from the first two PDEs (2.9a) leads to the formula

$$\frac{\partial}{\partial x}(\eta_1 v_1 + \eta_2 v_2) = 0,$$

which, under zero boundary conditions at infinity, yields

$$\frac{v_2}{v_1} = -\frac{\eta_1}{\eta_2}. \quad (2.15)$$

However, in the current manuscript, we do not make any *a priori* assumptions about boundary conditions; in particular, the relationship (2.15) is not used.

An important set of boundary conditions for solitary wave solutions is specified by the requirement of zero velocity shear at infinity, $|v_1 - v_2| \rightarrow 0$ as $x \rightarrow \pm\infty$. These boundary conditions are discussed in Section 6 below.

4) *Symmetry properties and traveling wave solutions.* It is evident that the symmetry group of the PDE system (2.9) includes translations in x and t , translation of the pressure by an arbitrary function of time, and the Galilei group:

$$\begin{aligned} x^* &= x + x_0 + Ct, & t^* &= t + t_0, & (v_i)^* &= v_i + C, & P^* &= P + P_0(t), \\ x_0, t_0, C &= \text{const.} \end{aligned} \quad (2.16)$$

The Galilei transformation can be used, for example, to set $V_1^- = 0$ in the boundary conditions (2.14), without loss of generality.

The space-time translation symmetry of the two-fluid system leads to the existence of the traveling wave solution ansatz, which is considered in detail in Section 3 below, and used for the construction of several families of exact solutions of the CC model in the following Sections 4 and 5.

An important property related with the symmetry structure of the two-fluid model (2.9), considered in Section 2.3, consists in an existence of equivalence transformations that lead to a dimensionless form and the reduction of the number of parameters.

2.3 The Dimensionless Form of the System; Parameter Reduction

The two-fluid system has been originally derived using dimensionless variables for the purpose of asymptotic comparisons, but presented in the dimensional form (2.9) containing five constant physical parameters

$$g, \rho_1, \rho_2, h_1, h_2. \quad (2.17)$$

We now derive a different dimensionless form of the PDE system (2.9), with a goal of minimization of the number of physical constants in the system. For this purpose, it is convenient to use the total channel depth $H = h_1 + h_2$ as the length parameter, and the quantity

$$\hat{Z} = \frac{h_1 - \zeta}{H} \equiv \frac{\eta_1}{H}, \quad 0 < \hat{Z} < 1, \quad (2.18)$$

as a dependent variable instead of ζ . The physical meaning of \hat{Z} is the relative depth of the top fluid level. Define the further dimensionless variables $\hat{x}, \hat{t}, \hat{v}_1, \hat{v}_2, \hat{P}$ by formulas

$$t = Q_t \hat{t}, \quad x = Q_h \hat{x}, \quad (2.19)$$

$$P(t, x) = Q_P \hat{P}(\hat{t}, \hat{x}), \quad v_i(t, x) = Q_i \hat{v}_i(\hat{t}, \hat{x}), \quad i = 1, 2.$$

The respective constants Q can be chosen so that the governing equations in terms of variables with hats will only involve *a single parameter*

$$S = \frac{\rho_1}{\rho_2}, \quad 0 < S < 1. \quad (2.20)$$

The scaling constants are given by

$$Q_h = H, \quad Q_t = \sqrt{\frac{H}{g}}, \quad Q_1 = Q_2 = \sqrt{gH}, \quad Q_P = \rho_1 g H, \quad (2.21)$$

and lead to the *dimensionless two-fluid system*, given by

$$\hat{Z}_{\hat{t}} + (\hat{Z} \hat{v}_1)_{\hat{x}} = 0, \quad (2.22a)$$

$$\hat{Z}_{\hat{t}} + (\hat{Z} \hat{v}_2)_{\hat{x}} - (\hat{v}_2)_{\hat{x}} = 0, \quad (2.22b)$$

$$\hat{v}_{1\hat{t}} + \hat{v}_1 \hat{v}_{1\hat{x}} - \hat{Z}_{\hat{x}} + \hat{P}_{\hat{x}} - \hat{Z} \hat{Z}_{\hat{x}} \hat{G}_1 - \frac{1}{3} \hat{Z}^2 \hat{G}_1_{\hat{x}} = 0, \quad (2.22c)$$

$$\hat{v}_{2\hat{t}} + \hat{v}_2 \hat{v}_{2\hat{x}} - \hat{Z}_{\hat{x}} + S \hat{P}_{\hat{x}} - \frac{1}{3} (1 - \hat{Z})^2 \hat{G}_2_{\hat{x}} + (1 - \hat{Z}) \hat{Z}_{\hat{x}} \hat{G}_2 = 0, \quad (2.22d)$$

$$\hat{G}_i \equiv \hat{v}_{i\hat{t}\hat{x}} + \hat{v}_i \hat{v}_{i\hat{x}\hat{x}} - (\hat{v}_{i\hat{x}})^2, \quad i = 1, 2.$$

The dimensionless form (2.22) is preferable to the original two-fluid equations (2.9), for example, in analyses involving classifications, such as symmetry and conservation law classifications, and stability analysis [21].

The ‘price’ paid for the reduction of the number of parameters is the loss of the apparent likeness between the pairs of equations (2.9) for each fluid layer. This similarity is, however, not perfect, in particular, due to the difference of signs in (2.9b). As a result, there is no ‘fluid interchange’ equivalence transformation that would exchange, for example, $(v_1, \rho_1) \leftrightarrow (v_2, \rho_2)$, $\zeta \leftrightarrow -\zeta$, etc.

Since the two-fluid system (2.9) is mapped into the dimensionless form (2.22) for any set of physical parameters (2.17), it follows that for the original system (2.9), there exist *equivalence transformations* [21, 24] that freely modify the parameters (2.17), while preserving the density ratio (2.20).

3 The Traveling Wave Reduction

3.1 The traveling wave ansatz

We start with a brief derivation of an ordinary differential equation describing bidirectional constant-speed traveling waves for the dimensionless two-fluid system (2.22). The existence of this important ansatz follows from the invariance of the PDEs (2.22) under the point transformations (2.16), and consequently, under a combined point symmetry with the generator

$$X = \hat{c} \frac{\partial}{\partial \hat{x}} + \frac{\partial}{\partial \hat{t}},$$

for an arbitrary dimensionless wave speed $\hat{c} = \text{const.}$ The invariants of X are all dependent variables of the problem, and the traveling wave coordinate

$$\hat{r} = \hat{r}(t, x) = \hat{x} + \hat{x}_0 - \hat{c}\hat{t} = \frac{1}{H}(x + x_0 - ct), \quad (3.1)$$

$\hat{x}_0 = \text{const.}$, $x_0 = H\hat{x}_0$, $c = \hat{c}\sqrt{gH}$. Traveling wave solutions of (2.22) are consequently sought in the form $\hat{Z}(\hat{t}, \hat{x}) = \hat{Z}(\hat{r})$, etc., leading to a system of four ODEs. This system can be reduced to a single first-order ODE; our derivation proceeds somewhat differently from the one in [1].

We note that due to the Galilei invariance of the model PDEs (2.9), without loss of generality, instead of using the full traveling wave ansatz, one may seek static solutions ($\hat{c} = 0$), and then convert them to traveling waves using the Galilei transformations (2.16) with an arbitrary traveling wave speed C . In the presentation below, however, we employ general formulas with $\hat{c} \neq 0$.

Within the current section, we use primes to denote the derivatives of the dependent variables \hat{Z} , \hat{v}_1 , \hat{v}_2 , \hat{P} with respect to \hat{r} . The substitution of the traveling wave ansatz into the first two ODEs of (2.22) yields

$$\hat{c}\hat{Z}' = (\hat{Z}\hat{v}_1)' = (\hat{Z}\hat{v}_2)' - \hat{v}_2'. \quad (3.2)$$

The general solution for the average velocity expressions is given by

$$\hat{v}_1 = \hat{c} + \frac{C_1}{\hat{Z}}, \quad \hat{v}_2 = \hat{c} + \frac{C_2}{1 - \hat{Z}}, \quad (3.3)$$

where C_1, C_2 are arbitrary constants. The dimensionless velocity expressions (3.3) are regular functions, since physically, $0 < \hat{Z} < 1$. Substituting (3.3) into the ODE version of (2.22c), one explicitly finds the pressure in terms of \hat{Z} :

$$\hat{P} = \hat{P}_0 + \hat{Z} - \frac{C_1^2}{6\hat{Z}^2} \left(2\hat{Z}\hat{Z}'' - (\hat{Z}')^2 + 3 \right), \quad \hat{P}_0 = \text{const.} \quad (3.4)$$

Using (3.3), (3.4) in the final ODE following from (2.22d) yields a rather complicated third-order ODE for $\hat{Z}(\hat{r})$, which we denote by $E_4[\hat{Z}] = 0$. To reduce its order, we seek conservation law multipliers (integrating factors) of this equation in the form $\Lambda = \Lambda(\hat{r}, \hat{Z})$, through the direct construction method (see, e.g., [18, 19, 21, 25–27]). Two integrating factors are immediately found, given by

$$\Lambda_1 = \hat{Z}^{-3}(1 - \hat{Z})^{-3}, \quad \Lambda_2 = \hat{Z}^{-2}(1 - \hat{Z})^{-3}.$$

The respective linearly independent first integrals satisfy

$$\Lambda_i E_4 = \frac{d}{d\hat{r}} \Phi_i[\hat{Z}], \quad i = 1, 2,$$

and are given by

$$\begin{aligned} \Phi_1[\hat{Z}] &= -\frac{1}{2\hat{Z}^2(1-\hat{Z})^2} \left[2\hat{Z}(1-\hat{Z})(\alpha_1\hat{Z} + \alpha_0)\hat{Z}'' \right. \\ &\quad \left. + (\alpha_0(1-2\hat{Z}) - \alpha_1\hat{Z}^2) \left(3 - (\hat{Z}')^2 \right) + 6(1-S)\hat{Z}^3(1-\hat{Z})^2 \right] \\ &= K_1 = \text{const}, \end{aligned} \quad (3.5)$$

$$\begin{aligned} \Phi_2[\hat{Z}] &= -\frac{1}{2\hat{Z}(1-\hat{Z})^2} \left[2\hat{Z}(1-\hat{Z})(\alpha_1\hat{Z} + \alpha_0)\hat{Z}'' \right. \\ &\quad \left. + (\alpha_1\hat{Z}(1-2\hat{Z}) + \alpha_0(2-3\hat{Z})) \left(3 - (\hat{Z}')^2 \right) + 3(1-S)\hat{Z}^3(1-\hat{Z})^2 \right] \\ &= K_2 = \text{const}, \end{aligned} \quad (3.6)$$

where the short-hand notation for constant combinations

$$\alpha_0 = C_1^2 S, \quad \alpha_1 = C_2^2 - \alpha_0 \quad (3.7)$$

has been used. In (3.5), (3.6), K_1 and K_2 are arbitrary constants corresponding to the choice of the boundary conditions of the original third-order ODE $E_4[\hat{Z}] = 0$. The two first integrals (3.5), (3.6) are now used to reduce the order of the ODE at hand by two. This can be done by substitution of \hat{Z}'' from one expression into the other, or by noticing that the linear combination $\Phi_1[\hat{Z}]\hat{Z} - \Phi_2[\hat{Z}]$ does not involve \hat{Z}'' . One arrives at the first-order ordinary differential equation

$$(\hat{Z}')^2 = \frac{A_4\hat{Z}^4 + A_3\hat{Z}^3 + A_2\hat{Z}^2 + A_1\hat{Z} + A_0}{\alpha_1\hat{Z} + \alpha_0} \equiv Q(\hat{Z}), \quad (3.8)$$

where

$$\begin{aligned} A_4 &= 3(1-S), \quad A_3 = 2K_1 - A_4, \\ A_2 &= -2(K_1 + K_2), \quad A_1 = 2K_2 + 3\alpha_1, \quad A_0 = 3\alpha_0. \end{aligned} \quad (3.9)$$

Overall, the family of ODEs (3.8) involves four independent constant parameters. For example, one may choose

$$\alpha_0 \geq 0, \quad \alpha_1, A_2, A_3 \in \mathbb{R}$$

as arbitrary constants. Then one has

$$A_1 = 3\alpha_1 - (A_2 + A_3 + A_4), \quad (3.10)$$

and the only additional restriction following from (3.7) is given by $\alpha_0 + \alpha_1 \geq 0$. The coefficient $A_4 > 0$ is physically defined by the fluid density ratio S according to (2.20). Further, for a nontrivial flow in which the average velocities (3.3) are not constant at the same time, one requires $C_1 C_2 \neq 0$, hence the denominator of (3.8) does not vanish.

The physical solution additionally depends on the arbitrary constant parameter \hat{c} . In terms of α_0 , α_1 , \hat{c} , S , the dimensionless velocities are given by

$$\hat{v}_1 = \hat{c} \pm \frac{\sqrt{\alpha_0/S}}{\hat{Z}}, \quad \hat{v}_2 = \hat{c} \pm \frac{\sqrt{\alpha_0 + \alpha_1}}{1 - \hat{Z}}, \quad (3.11)$$

where the signs \pm can be independently chosen in both velocity expressions to yield independent solutions of the two-fluid model. Indeed, it is straightforward to verify that the model equations (2.9) are satisfied for any velocity expressions arising from (3.3) with C_1 , C_2 satisfying (3.7).

3.2 The ordinary differential equation (3.8)

The nonlinear autonomous ODE (3.8) with a rational right-hand side $Q(\hat{Z})$ does not belong to any well-studied ODE class, and a closed form of its general solution is not known. A dimensional ODE analogous to (3.8) with a rational right-hand side appeared in [6] for the case of steady solitary waves. The zeroes of the numerator of the right-hand side were analyzed in [1] using a diagram which established parameter ranges and appropriate initial conditions to numerically produce solitary wave-type solution curves, which were argued to compare well with experimental data of [28]. In [17, 29], further analysis led to finding appropriate conditions for numerical kink and periodic traveling wave solutions. Numerical comparisons of [17] between the solutions of the full Euler equations for the two-fluid channel, the two-fluid approximate model, and the KdV equation demonstrated a reasonable agreement between the first two models, and a relatively poor approximation provided by the latter.

An implicit general solution of (3.8) is readily written,

$$\pm \int^{\hat{Z}} Q(s)^{-1/2} ds = r - r_0, \quad (3.12)$$

(see, e.g., [6]), but is not useful for practical computations. A similar but different family of nonlinear ODEs was studied in [30]; in that work, the integral analogous to the left-hand side of (3.12) was evaluated in terms of general elliptic functions, the solution still remaining implicit.

It is easy to see the ODE (3.8) can be mapped into an equation with a polynomial right-hand side, as follows. Firstly, if $\alpha_1 \neq 0$, then without loss of generality, the transformation $Y(\hat{r}) = (\hat{Z} - \alpha_0/\alpha_1)^{-1}$ maps (3.8) to an ODE with the fifth-degree polynomial right-hand side

$$(Y')^2 = \frac{A_0}{\alpha_1} Y^5 + \frac{A_1}{\alpha_1} Y^4 + \frac{A_2}{\alpha_1} Y^3 + \frac{A_3}{\alpha_1} Y^2 + \frac{A_4}{\alpha_1} Y. \quad (3.13)$$

Alternatively, if $\alpha_1 = 0$, the right-hand side of the ODE (3.8) has the fourth degree polynomial form as it stands. Moreover, if there is a common root for the numerator and denominator of the right-hand side of (3.8), the ODE (3.8) has a cubic polynomial right-hand side, and belongs to a class of Jacobi-like equations; e.g., [2].

Multiple exact solutions of the ODE (3.8) can be constructed by inspection that do not correspond to exact solutions of the two-fluid equations (2.9), since they lead to the violation of physical conditions, such as the stratification requirements $S < 1$, the interface displacement domain $-h_2 < \zeta < h_1$, etc. In subsequent Sections 4 and 5, we derive exact, explicit, closed-form expressions for several classes of solutions of the ODE (3.8), leading to physically meaningful

solutions of the two-fluid equations (2.9). The solutions are expressed in terms of elementary functions; they satisfy specific physically appropriate boundary conditions. Other exact solution formulas involving elementary functions can be derived in a similar fashion, in particular, ones that exhibit singular behaviour. We do not list them since they do not correspond to physical motions of the two-fluid system.

4 Exact Closed-Form Cnoidal and Solitary Wave Solutions

Solitary and cnoidal waves are known to exist for the Korteweg-de Vries equation and a number of other nonlinear models. We show that physical solutions of such kinds also arise from the Camassa-Choi traveling wave ODE (3.8). The following theorem holds.

Theorem 4.1. *The family of ODEs (3.8) admits exact solutions in the form*

$$\hat{Z}(\hat{r}) = B_1 \operatorname{sn}^2(\gamma \hat{r}, k) + B_2, \quad (4.1)$$

for arbitrary constants k, B_1, B_2 . The remaining constants γ and $\alpha_{1,2}$ are given by one of the two relationships (A.1), (A.2) listed in Appendix A.

Theorem 4.1 is proven by a direct substitution. One consequently has *two families* of exact solutions of the dimensionless two-fluid system (2.22), each depending on the arbitrary constants k, B_1, B_2, \hat{c} , as well as arbitrarily prescribed physical parameters $S = \rho_1/\rho_2, h_1, h_2, g$. The dimensional solutions of the two-fluid system (2.9) are computed as follows. First, as per the definition of \hat{Z} in (2.18) and the formula (4.1), one has

$$\zeta(x, t) = h_1 - H\hat{Z} = (h_1 - HB_2) - HB_1 \operatorname{sn}^2(\gamma \hat{r}(x, t), k). \quad (4.2)$$

For both solution families, the pressure, according to (2.19), (2.21), (3.4), is given by

$$P(x, t) = \rho_1 g H \hat{P}(\hat{r}(x, t)). \quad (4.3)$$

The dimensional average velocities have different expressions for the two cases that arise.

Case 1. For the relationship (A.1) between the solution parameters, one has $\alpha_0 + \alpha_1 = C_2^2 = 0$. The mean-layer velocities computed from (3.3) and (2.19) are given by

$$v_1(x, t) = \sqrt{gH} \left(\hat{c} \pm \frac{\sqrt{\alpha_0/S}}{B_1 \operatorname{sn}^2(\gamma \hat{r}(x, t), k) + B_2} \right), \quad v_2(x, t) = \hat{c} \sqrt{gH} = \text{const}, \quad (4.4)$$

where different choices of the sign yield different admissible forms of $v_1(x, t)$.

Case 2. For the second parameter relationship (A.2), one has $C_1 = \alpha_0 = 0$, $C_2 = \pm\sqrt{\alpha_1}$, the solution has a constant upper fluid layer-average velocity $v_1(x, t)$ and two possible expressions for $v_2(x, t)$:

$$v_1(x, t) = \hat{c} \sqrt{gH} = \text{const}, \quad v_2(x, t) = \sqrt{gH} \left(\hat{c} \pm \frac{\sqrt{\alpha_1}}{1 - B_1 \operatorname{sn}^2(\gamma \hat{r}(x, t), k) - B_2} \right). \quad (4.5)$$

Remark 1. The constant value of a corresponding layer-average velocity $v_i = \text{const}$ in Cases 1 and 2 above implies, through the asymptotic expression (2.13), that the corresponding horizontal fluid velocity component $u_i(t, x, z) = O(\epsilon^4)$. We note that in the papers [1, 17] where solitary wave profiles were obtained numerically, the behaviour of the layer-average velocities was not discussed.

Remark 2. In order to describe elevation or depression wave trains positioned directly above or below the fluid interface $\zeta = 0$, one can choose

$$B_2 = \frac{h_1}{H} - B_1. \quad (4.6a)$$

This leads to the interface displacement formula

$$\zeta(x, t) = HB_1 \text{cn}^2(\gamma \hat{r}(x, t), k). \quad (4.6b)$$

4.1 Periodic cnoidal waves

Periodic cnoidal-type solutions of the two-fluid system (2.9) arise from the formula (4.1) for $0 < k < 1$. The period of the elliptic sine $\text{sn}(x, k)$ is given by

$$\tau = \frac{2\pi}{M(1, \sqrt{1-k^2})}, \quad (4.7)$$

where $M(a, b)$ denotes the Gauss' algebraic-geometric mean of a, b ; for the function $\text{sn}^2(x, k)$, the period equals $\tau/2$. The dimensionless and the dimensional wavelength of the exact solutions arising from (4.1) are consequently given by

$$\hat{\lambda} = \frac{\pi}{\gamma M(1, \sqrt{1-k^2})}, \quad \lambda = H\hat{\lambda}. \quad (4.8)$$

For the cnoidal wave solutions (4.1), $\gamma = \gamma(B_1, B_2, k)$ according to (A.1) or (A.2). In particular, γ is independent of the fluid densities since it does not involve the density ratio S . Sample plots of $\gamma(B_1, k)$ in Case 1 (formulas (A.1)), for the choice of B_2 according to (4.6a), with $h_1/H = 2/5$, are given in Figure 2. The limit $k \rightarrow 1^-$, $\hat{\lambda} \rightarrow +\infty$ corresponds to the cnoidal-solitary wave transition.

Sample plots of exact solutions ζ , v_1 , v_2 , P of the two-fluid system (2.9), as functions of dimensionless spatial coordinate x/λ , are presented in Figure 3 for the parameter values

$$\hat{c} = 1, \quad h_1 = 0.4 \text{ m}, \quad h_2 = 0.6 \text{ m}, \quad H = 1 \text{ m}, \quad g = 9.8 \text{ m/s}^2, \quad x_0 = t = 0, \quad (4.9a)$$

and the density ratio

$$S = 0.9. \quad (4.9b)$$

for a set of values of k , $0 < k < 1$, and B_1 . The above choice of parameters \hat{c}, H corresponds to the dimensional wave speed $c = \hat{c}\sqrt{gH} \simeq 3.13 \text{ m/s}$. Formulas (4.3), (4.4), (4.5), (4.6b) are used; in (4.4) and (4.5), positive signs are chosen. The four black curves in Figure 3 correspond to Case 1 solutions plotted for $B_1 < 0$, and represent periodic surface depression waves, with constant layer-average horizontal speed of the lower fluid. The dashed blue curves for Case 2

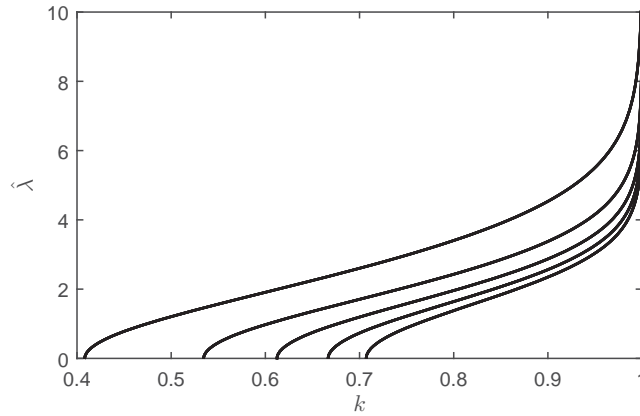


Figure 2: Dependence of the dimensionless wavelength $\hat{\lambda}$ of the special cnoidal wave (4.6) on the elliptic function parameter k , for $h_1/H = 2/5$, for Case 1 (formulas (A.1)). From top to bottom: curves for $B_1 = -0.4, -0.32, -0.24, -0.16, -0.08$.

solutions are shown for $B_1 > 0$, corresponding to surface elevations, and constant layer-average horizontal speed values of the upper fluid. The plotted curves correspond to the values of (k, B_1) pairs and wavelengths given in Table 1. We note that despite of the same values of the amplitude of the elliptic cosine, $|B_1|$, the solutions curves for Case 1 and Case 2 are not symmetric. In particular, the last, dimensional plot in Figure 3 shows that the wavelengths of the oscillations are different; this is due to the difference of the expressions for α_1 in Case 1 and Case 2, with k, B_1 taken the same for both cases.

Figure 4 shows sample flood diagrams for the horizontal velocities $u_i(t, x, z)$ computed through the asymptotic formulas (2.13) for the cnoidal wave solutions (4.6b) (Cases 1 and 2).

Remark 3. Depending on the choice of free parameters listed in Theorem 4.1, exact solutions of the CC model given by formulas (4.1), (4.3), (4.4), (4.5) may or may not satisfy the asymptotic requirement $\epsilon \ll 1$ (2.5). Choosing values of k closer to 1, one can unboundedly increase the wavelength $\lambda = L$ (4.8). Exact solutions of both small and large amplitude exist within the indicated class. Some examples are provided in Table 1, which contains parameter values used to produce Figures 3 and 4.

Case	k	B_1	λ , m	$\epsilon = H/\lambda$
1	0.9990	-0.0300	15.7055	0.0637
2	0.9990	0.0300	90.4410	0.0111
1	0.9900	-0.1000	6.8466	0.1461
2	0.9900	0.1000	22.0327	0.0454
1	0.9000	-0.1800	3.2188	0.3107
2	0.9000	0.1800	7.1438	0.1400
1	0.8000	-0.2500	1.9146	0.5223
2	0.8000	0.2500	3.1912	0.3134
1	0.9900	-0.2500	5.2898	0.1890

Table 1: Sample exact solution parameters and wavelengths for the exact periodic cnoidal wave solutions (4.1).

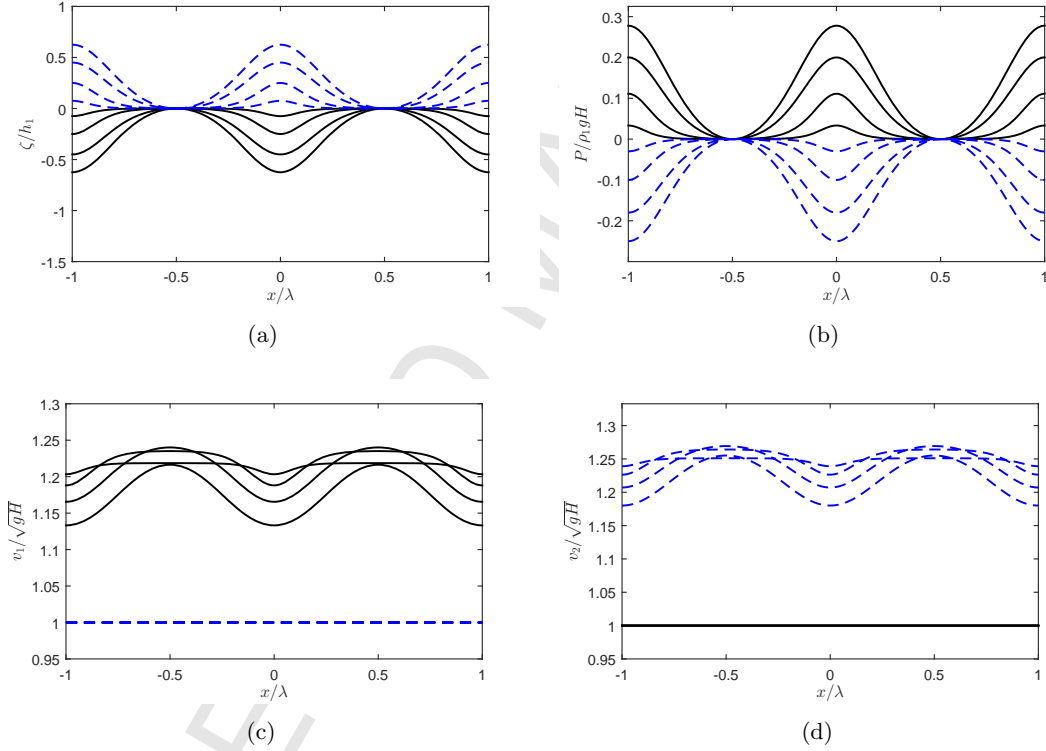


Figure 3: Dimensionless flow parameter curves for the periodic cnoidal wave exact solution family (4.3), (4.4), (4.5), (4.6b). Case 1 curves are shown in solid black, with amplitudes $B_1 < 0$ (Table 1, rows 1, 3, 5, 7); Case 2 curves are dashed blue, $B_1 > 0$ (small to large amplitude, Table 1, rows 2, 4, 6, 8). (a): the dimensionless interface displacement; (b) the dimensionless pressure at the interface; (c), (d): the dimensionless average horizontal velocities of the upper and the lower fluid. The actual (dimensional) spatial wavelengths of the presented solutions are not equal; they are given in Table 1.

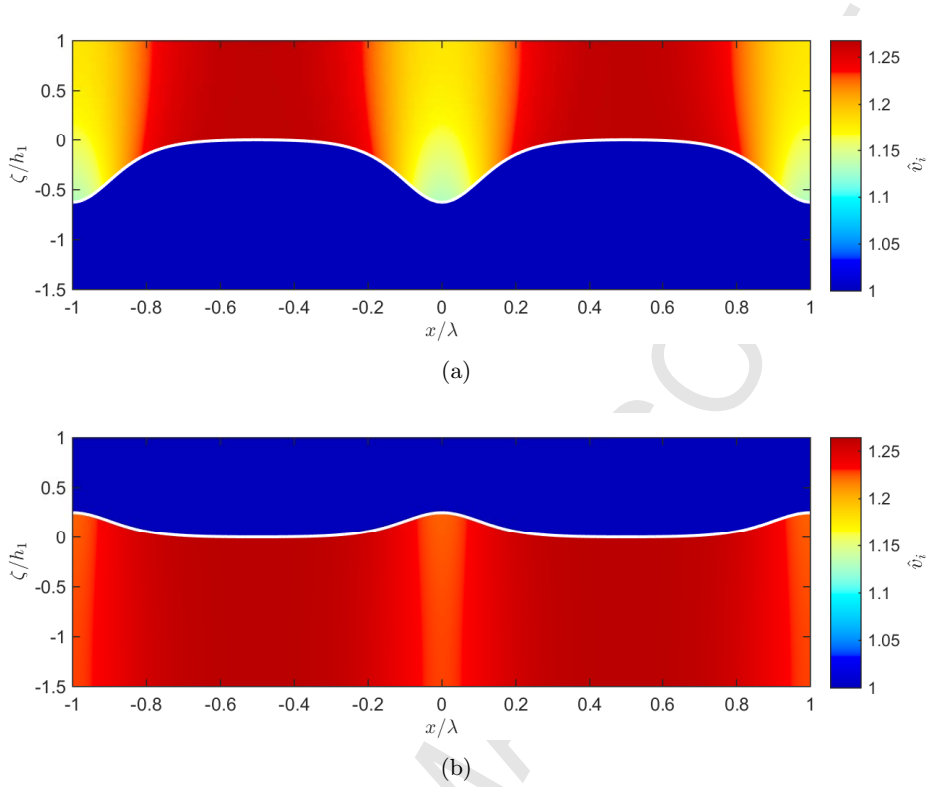


Figure 4: Flood diagrams for the right-propagating cnoidal wave solutions (4.1), showing dimensionless values of the fluid interface displacement (white curve) and the (x, z) -dependent horizontal velocities u_i computed through the formulas (2.13). Figures are given for the solution parameters (4.9) with (a) $k = 0.99$, $B_1 = -0.25$ for Case 1, and (b) $k = 0.99$, $B_1 = 0.1$ for the Case 2 solution. The corresponding dimensional spatial wavelengths are given in Table 1.

4.2 Solitary waves

For both Case 1 and Case 2, solitary waves arise from the solution (4.1) for $k = 1$, since $\text{sn}^2(y, 1) = \tanh^2 y = 1 - \cosh^{-2} y$, and

$$\hat{Z}(\hat{r}) = (B_1 + B_2) - B_1 \cosh^{-2}(\gamma \hat{r}). \quad (4.10)$$

Solutions corresponding to Case 1 describe propagating fluid interface depression waves, whereas Case 2 corresponds to the elevation waves. Coefficient formulas (A.1), (A.2) still hold when $k = 1$. The solution family (4.3), (4.4), (4.5), (4.10) depends on the arbitrary parameters B_1 , B_2 , \hat{c} , the physical parameters $S = \rho_1/\rho_2$, h_1 , h_2 , g , and on the sign choice in the average velocity expressions (4.4), (4.5). It is natural to choose B_2 according to the formula (4.6a):

$$\zeta(x, t) = HB_1 \cosh^{-2}(\gamma \hat{r}(x, t)); \quad (4.11)$$

then $\zeta \rightarrow 0$ as $x \rightarrow \pm\infty$.

In Figure 5, sample right-propagating depression and elevation-type solitary wave exact solution profiles are shown for channel/fluid parameters (4.9), for $B_1 = -0.05, -0.15, -0.25$ (Case 1)

and $B_1 = 0.05, 0.15, 0.25$ (Case 2), and B_2 given by (4.6a). In formulas (4.4) and (4.5), positive signs are chosen.

As in the periodic case, for the solitary wave solution family, one of the layer-average velocity values is constant. Sample plots of the approximate actual (non-average) horizontal velocity values $u_i(t, x, z)$, calculated through the asymptotic formulas (2.13) in a moving frame, are shown in flood diagrams in Figure 6.

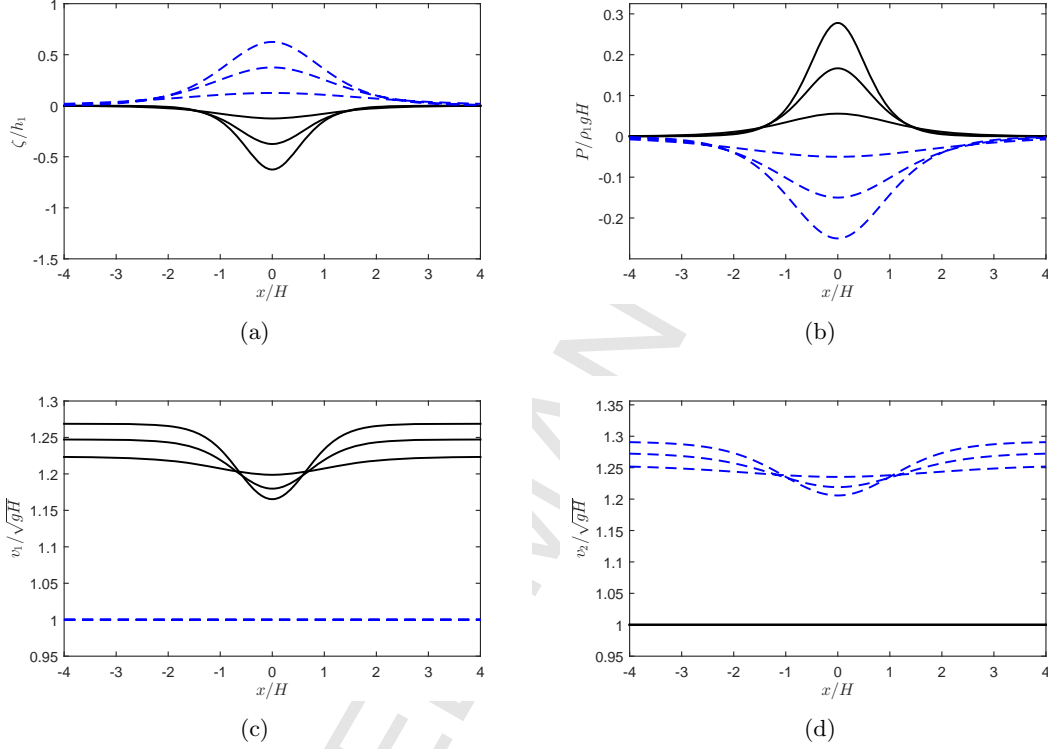


Figure 5: Dimensionless flow parameter curves for the right-propagating solitary wave exact solution families (4.3), (4.4), (4.5), (4.10). Case 1 curves are shown in solid black, with amplitudes $B_1 = -0.05, -0.15, -0.25$; Case 2 curves are dashed blue, for $B_1 = 0.05, 0.15, 0.25$ (small to large amplitude). In this figure, the dimensionless spatial coordinate is the one normalized by the total channel depth: x/H . (a): dimensionless interface displacement; (b) dimensionless pressure at the interface; (c), (d): dimensionless average horizontal velocities of the upper and the lower fluid.

We are now interested in a relationship between the wave amplitude and the typical wavelength of the exact solitary wave solutions (4.10). The argument of the hyperbolic cosine is $\gamma \hat{r} \sim \gamma x/H$, hence one defines the dimensional wavelength as

$$\lambda_s = \frac{H}{\gamma(B_1, B_2)}. \quad (4.12)$$

We use $\lambda_s^{(1)}, \lambda_s^{(2)}$ to denote the wavelengths (4.12) arising for Cases 1 and 2 (formulas (A.1) and

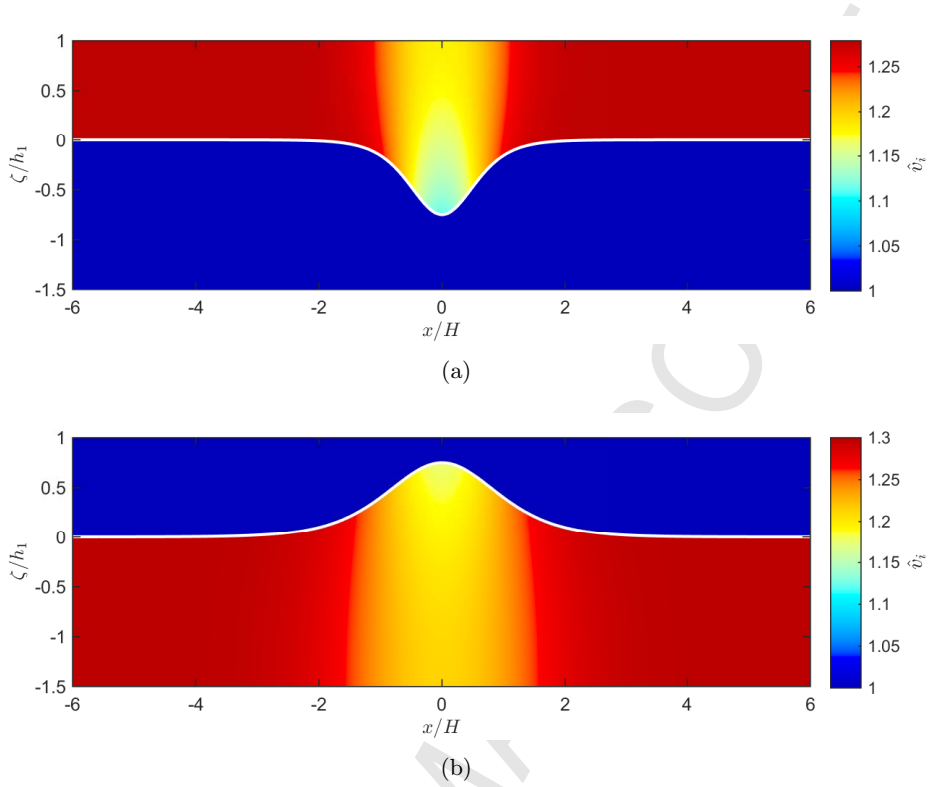


Figure 6: Flood diagrams for the solitary wave solutions (4.10), showing dimensionless values of the fluid interface displacement (white curve) and the (x, z) -dependent horizontal velocities u_i computed through the formulas (2.13). Figures are given for the solution parameters (4.9) with (a) $B_1 = -0.3$, Case 1; and (b) $B_1 = 0.3$, Case 2. The spatial coordinate is the one normalized by the total fluid height: x/H .

(A.2)), respectively.

Denote the fluid depth ratio

$$R = \frac{h_1}{h_2}. \quad (4.13)$$

In [28], for $R = 5.09$ and the density ratio $S = 0.63$, for solitary waves of elevation, experimental measurements of the dimensionless wavelength λ_s/h_2 versus the dimensionless wave amplitude a/h_2 were presented. We consider a similar wavelength-amplitude relationship for the exact solitary wave solutions (4.11).

For the elevation-type solitary waves (Case 2, $B_1 > 0$), let B_2 be given by the formula (4.6a) (or, in general, by $B_2 = \text{const} - B_1$), to yield amplitude-independent fluid depths. The elevation amplitude is given by $a = HB_1$. Using (A.2), it is straightforward to show that the dimensionless wavelength-amplitude relationship is given by

$$\hat{\lambda}_s^{(2)} = f(q) = \frac{2}{\sqrt{3}} \sqrt{1 + q^{-1}}, \quad (4.14)$$

were $\hat{\lambda}_s^{(2)} = \lambda_s^{(2)}/h_2$, $q = a/h_2$. Interestingly, the relationship (4.14) is independent of both the fluid density ratio S and the fluid depth ratio R .

For the depression-type exact solitary wave solutions (Case 1, $B_1 < 0$), with the same choice of B_2 , the amplitude is defined as $a = H|B_1|$. The expression for $\lambda_s^{(1)}/h_2$ as a function of a/h_2 does not turn out elegant, in particular, it is dependent on the fluid depths. However, using the upper fluid depth h_1 for non-dimensionalization, and denoting $\hat{\lambda}_s^{(1)} = \lambda_s/h_1$, $q' = a/h_1$, one arrives at the *same formula* $\hat{\lambda}_s^{(1)} = f(q')$ as (4.14). This is another manifestation of the partial “fluid interchange” symmetry mentioned earlier.

In Figure 7, a plot of the wavelength-amplitude relationship (4.14) is shown.

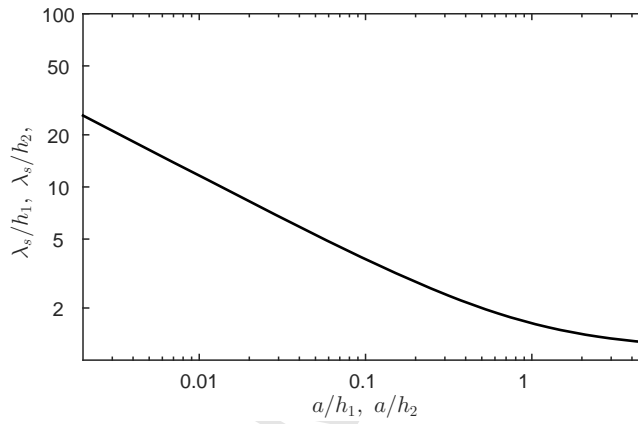


Figure 7: The dimensionless wavelength-amplitude relationship $\hat{\lambda}_s = f(q)$ (4.14) for the exact solitary wave solutions (4.10). Here $q = a/h_1$ and $a = H|B_1|$ for depression waves (Case 1), and $q = a/h_2$, $a = HB_1$ for elevation waves (Case 2).

5 The Second Family of Exact Closed-Form Solutions: Periodic and Kink-type Waves

Further families of exact solutions of the two-fluid model arise from the traveling wave ODE (3.8) as follows.

Theorem 5.1. *The ODE (3.8) admits exact solutions in the form*

$$\hat{Z}(\hat{r}) = \frac{B_1}{\text{sn}(\gamma \hat{r}, k) + B_2}, \quad (5.1)$$

for arbitrary constants B_1, B_2, S . The remaining constants γ, k , and $\alpha_{1,2}$ are given by any one of the three relationships (B.1), (B.2), (B.3) listed in Appendix B.

The above result is also verified by a direct substitution of (5.1) into the ODE (3.8). One consequently has three families of exact solutions of the dimensionless two-fluid system (2.22),

each depending on *three arbitrary constant parameters* B_1, B_2, \hat{c} , as well as on the arbitrarily prescribed channel/fluid parameters $S = \rho_1/\rho_2$, h_1 , h_2 and the free fall acceleration g .

The solution families arising from (5.1) are regular and physically meaningful when $|B_2| > 1$, $0 < \hat{Z}(\hat{r}) < 1$. The dimensional fluid interface position $\zeta(x, t)$ and the flow parameters $v_1(t, x)$, $v_2(t, x)$, $P(t, x)$ are found from (2.18), (2.19), (3.3), (3.4). They are essentially different from those described in Section 4. Ranges of parameters exist that satisfy the asymptotic requirement (2.5).

Case 1. For the coefficient relationship (B.1), $\alpha_0 + \alpha_1 = C_2 = 0$, and hence, similarly to (4.4), the mean velocity of the bottom layer $v_2(t, x) = \text{const}$.

Case 2. For the relationship (B.2), $\alpha_0 = C_1 = 0$, which yields the constant mean velocity of the top layer, $v_1(t, x) = \text{const}$ (cf. (4.4)).

Case 3. For the solution family determined by (B.3), both mean horizontal velocities are non-constant.

From the period formula (4.7), the dimensionless and the dimensional x -wavelength of exact solutions arising from (5.1) are computed as follows:

$$\hat{\lambda} = \frac{2\pi}{\gamma M(1, \sqrt{1-k^2})}, \quad \lambda = H\hat{\lambda}. \quad (5.2)$$

For the periodic solutions (5.1), the parameters γ and k are functions of B_1 , B_2 , and do not depend on the density ratio S . In particular, for Case 3, one has $k = 1/\gamma$, and

$$\hat{\lambda}(k) = \frac{2\pi k}{M(1, \sqrt{1-k^2})}, \quad (5.3)$$

which is plotted in Figure 8. The limit $k \rightarrow 1^-$, $\hat{\lambda} \rightarrow +\infty$ corresponds to the cnoidal-kink wave transition. Periodic and kink-type traveling wave exact solutions are discussed in Sections 5.1 and 5.2 below.

5.1 Periodic Solutions with Nonconstant Velocities

As a first illustration, we compute periodic solutions to the CC model (2.9) in the form (5.1), (B.3), that is, in Case 3. Choose the physical constants

$$\hat{c} = 1, \quad h_1 = 3/7 \text{ m}, \quad h_2 = 4/7 \text{ m}, \quad H = 1 \text{ m}, \quad g = 9.8 \text{ m/s}^2, \quad x_0 = t = 0, \quad S = 0.9. \quad (5.4)$$

B_1	B_2	k	λ , m	$\epsilon = H/\lambda$
2.3995	5	0.9950	20.4057	0.0980
2.3881	5	0.8996	11.3073	0.1769
2.3037	5	0.6000	5.5882	0.3579

Table 2: Sample exact solution parameters and wavelengths for the exact periodic cnoidal wave solutions (5.1).

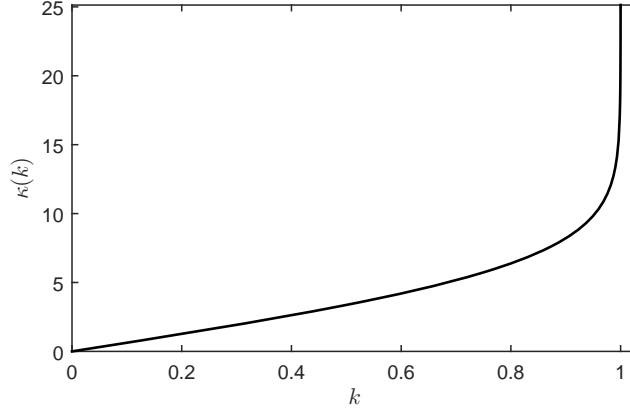


Figure 8: The dimensionless wavelength $\hat{\lambda}(k)$ (5.3) for the periodic traveling wave solutions (5.1), Case 3.

Solution curves in Figure 9 are plotted for a set of arbitrary constants B_1, B_2 and the resulting values of k and the spatial wavelength λ are given in Table 2. For the chosen sample parameters, surface wave amplitudes are rather similar, therefore, a dimensional plot of the fluid interface displacement is shown. The flood diagram in Figure 10 shows a snapshot the horizontal velocity values $u_i(t, x, z)$ (2.13) for the parameters in the second row of Table 2. Figures 9, 10 were produced under the positive sign choice for both average velocities in (3.11).

5.2 Kink/Anti-Kink Solutions of the Two-Fluid Equations

Since $\text{sn}(y, 1) = \tanh y$, one readily constructs exact kink- and anti-kink-type solutions of the two-fluid PDE system (2.9)

$$\hat{Z}(\hat{r}) = \frac{B_1}{\tanh(\gamma \hat{r}) + B_2} \quad (5.5)$$

by setting $k = 1$ in formulas (5.1), (B.1), (B.2), (B.3). Physically meaningful solutions exist, satisfying, in particular, the condition $0 < \hat{Z}(\hat{r}) < 1$.

As an illustration, we consider Case 3, and the coefficient formulas (B.3) with $k = 1$. This yields, in particular, the following relationships between an arbitrary constant B_1 and other solution parameters:

$$\begin{aligned} B_2^2 - 2B_1B_2 - 1 &= 0, & \gamma^2 &= \frac{3}{B_1^2}, & \alpha_1 &= 0, \\ \alpha_0 &= \frac{A_4B_1^2(2B_2 - B_1)}{12(6B_1^2B_2 + 3B_1 + 2B_2)}. \end{aligned} \quad (5.6)$$

The relationships (5.6) lead to physical solutions (other relationships exist, in particular, other admissible forms of B_2 , leading to singular solutions). From (5.6), $B_2 = B_1 \pm \sqrt{B_1^2 + 1}$; regular solutions arise with the positive sign choice when $B_1 > 0$ and the negative sign choice when $B_1 <$

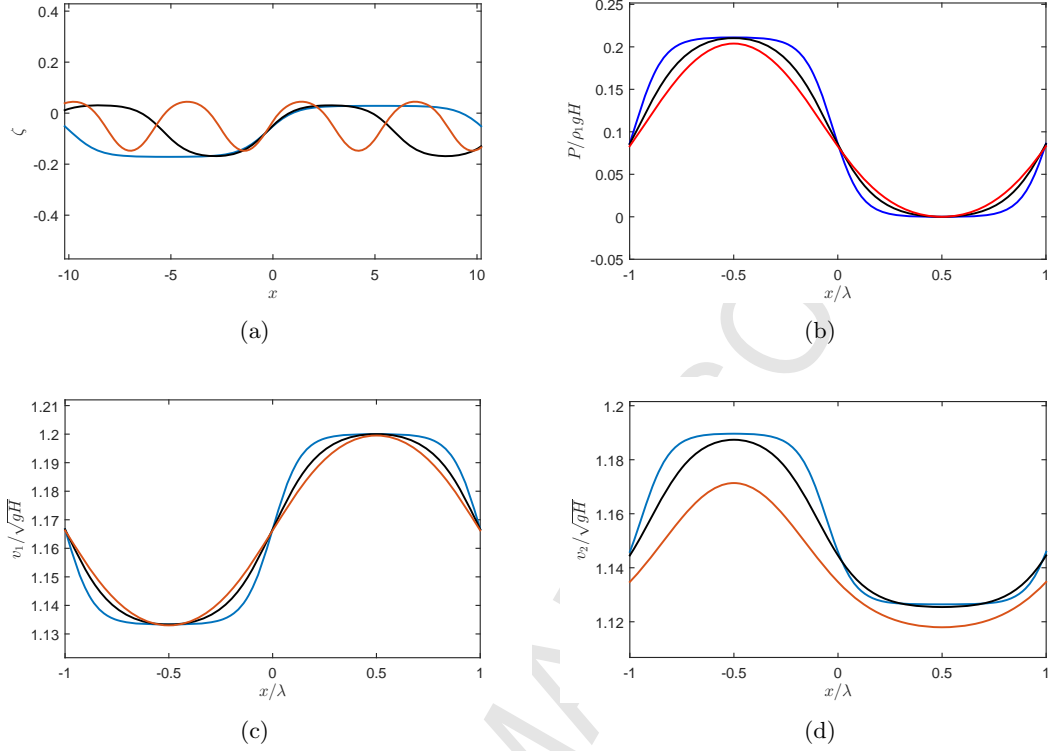


Figure 9: Sample flow parameter curves for the exact periodic solutions (5.1) of the Camassa-Choi model, Case 3, in the case of right-propagating waves. Curve colors blue, black, and red correspond to the three rows of Table 2. (a): dimensional interface displacement; (b) dimensionless pressure at the interface; (c), (d): dimensionless average horizontal velocities of the upper and the lower fluid.

0. The dimensional amplitude and the characteristic wavelength of the interface displacement for the kink/anti-kink solutions are readily computed from (2.18), (5.5), (5.6), and are given by

$$a = H|B_2|^{-1}, \quad \lambda = \frac{H}{\gamma} = \frac{H|B_1|}{\sqrt{3}}. \quad (5.7)$$

We note that for (5.6), in the limiting case $B_1 \rightarrow \pm\infty$, the larger root $B_2 \simeq 2B_1$, and the kink/anti-kink solutions tend to a constant: $\hat{Z}(\hat{r}) \rightarrow 1/2$, corresponding to an equilibrium situation in a channel with equal fluid layer thicknesses $h_1 = h_2$.

Plots of sample curves of right-propagating kink-type exact solutions, for dimensionless parameters given in Table 3 and physical constants

$$\hat{c} = 1, \quad h_1 = h_2 = 0.5 \text{ m}, \quad H = 1 \text{ m}, \quad g = 9.8 \text{ m/s}^2, \quad x_0 = t = 0, \quad S = 0.9, \quad (5.8)$$

and the flood velocity plot corresponding to the second row of Table 3, are shown in Figures 11, 12, for the choice of the positive sign of γ in (5.6).

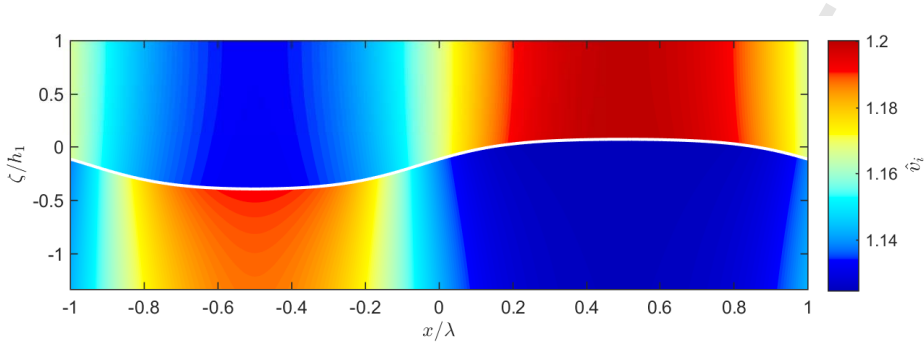


Figure 10: A flood diagram for one period of a right-propagating cnoidal wave solution (5.1), showing dimensionless values of the fluid interface displacement (white curve) and the (x, z) -dependent horizontal velocities u_i computed through the formulas (2.13), for the solution parameters in the second row of Table 2.

B_1	B_2	a	λ	$\epsilon = H/\lambda$
2	4.2361	0.8660	1.1547	0.8660
5	10.0990	0.3464	2.8868	0.3464
15	30.0333	0.1155	8.6603	0.1155
-3	-6.1623	0.5774	1.7321	0.5774
-6	-12.0828	0.2887	3.4641	0.2887
-24	-48.0208	0.2887	13.8564	0.0722

Table 3: Sample exact solution parameters for the kink/anti-kink exact solutions (5.5).

6 Exact Traveling Wave Solutions and the Condition for No Velocity Shear at Infinity

6.1 Solitary Wave Solutions

The work of Choi and Camassa [1], as well as many other papers on the subject, deals exclusively with traveling wave-type finite fluid interface perturbations corresponding to the zero boundary conditions at infinity:

$$\zeta, |v_1 - v_2| \rightarrow 0 \text{ as } x \rightarrow \pm\infty. \quad (6.1)$$

In general, the relationship between depth and density ratios can be defined using the ratio parameter β ,

$$R = \beta\sqrt{S}, \quad (6.2)$$

with $0 < \beta < 1$, $\beta = 1$, and $\beta > 1$ corresponding to subcritical, critical, and supercritical cases, respectively. For solitary waves of the two-fluid model (2.9), as well as for the general

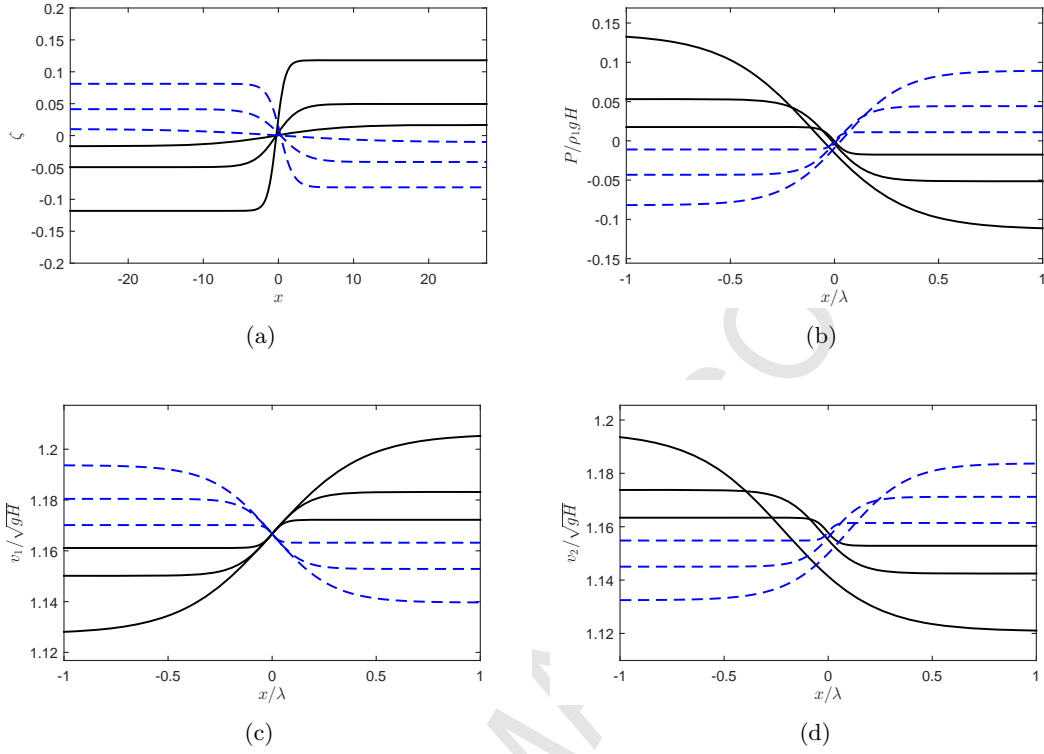


Figure 11: Sample flow parameter curves for right-propagating kink/anti-kink solutions (5.5) of the Camassa-Choi model. Black solid curves (large to small amplitude) correspond to the first three rows of Table 3 (kink solutions). Blue dashed curves (large to small amplitude) correspond to the rows 4-6 of Table 3 (anti-kink solutions). (a): dimensional interface displacement; (b) dimensionless pressure at the interface; (c), (d): dimensionless layer-average horizontal velocities of the upper and the lower fluid.

Green-Naghdi systems, the critical depth ratio

$$R_c = \left(\frac{h_1}{h_2} \right)_c = \left(\frac{\rho_1}{\rho_2} \right)^{1/2} = \sqrt{S}. \quad (6.3)$$

plays an important role [1, 23]. In particular, for the two-fluid equations (2.9), at the critical depth ratio, solitary wave-type solutions have been shown to not exist [1].

Under the no-shear conditions (6.1), the velocity formulas (3.3) in the traveling wave framework yield

$$C_1 = -\hat{c}B_2, \quad C_2 = \hat{c}(B_2 - 1). \quad (6.4)$$

The dimensionless average velocities and pressure are given by the expressions (3.3) and (3.4), where the dimensionless displacement function \hat{Z} satisfies the ODE (3.8) with parameters restricted by the condition (6.1).

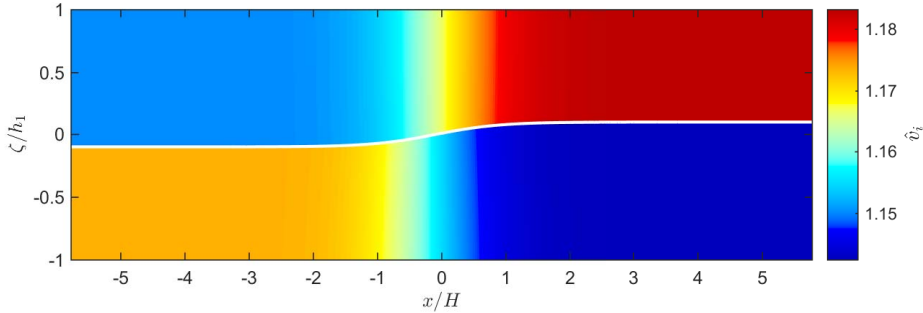


Figure 12: A flood diagram for the kink solution (5.5), showing dimensionless values of the fluid interface displacement (white curve) and the (x, z) -dependent horizontal velocities u_i computed through the formulas (2.13) for the parameters listed in (6.7) and the second row of Table 3.

As discussed in Section 3.2, the general closed-form solution of the ODE (3.8) is not available; in [1], solitary wave-type solution profiles satisfying (6.1) have been obtained by numerical integration. A family of solitary wave exact solutions (4.10), (4.11) of the ODE (3.8) has been derived in Section 4. A direct computation shows that there do exist ranges of parameters B_1, B_2 for which the exact solutions (4.10) of the ODE (3.8) satisfy the boundary conditions (6.1), however, all such solutions fail to satisfy the boundedness condition (2.18), and are therefore non-physical. It follows that the solutions numerically computed in [1] do not belong to the exact solution family (4.10).

Specifically, for the exact solutions (4.10) with (4.6a), the dimensionless velocity shear values at infinity $|\Delta\hat{v}|_\infty = |\hat{v}_1 - \hat{v}_2|_{x=\pm\infty}$ are readily computed. They are given by

$$|\Delta\hat{v}|_\infty^{(1)} = \sqrt{\frac{1-S}{S} \left(\frac{h_1}{H} - B_1 \right)}, \quad |\Delta\hat{v}|_\infty^{(2)} = \sqrt{(1-S) \left(\frac{h_2}{H} + B_1 \right)} \quad (6.5)$$

for the Cases 1 and 2, respectively. From the physical conditions $-h_2 < HB_1 < h_1$ on the interface displacement amplitude in (4.11), it follows that the velocity shear values at infinity never vanish for the presented solitary wave-type solutions. In both cases, a specification of an admissible velocity shear value prescribes the wave amplitude parameter B_1 through (6.5).

6.2 Kink/Anti-Kink Solutions

We now examine the possibility for the members of the second family of exact traveling wave solutions found in this paper (Section 5) to satisfy zero boundary conditions at infinity. In particular, for the kink/anti-kink solutions (5.5), one can require that the velocity shear must vanish at one of the infinities. Requiring $|v_1 - v_2| \rightarrow 0$ as $x \rightarrow \infty$ or $x \rightarrow -\infty$ in the exact solution (5.1), one obtains, respectively, the following restrictions on the velocity constants:

$$C_2 = C_1 \left(\frac{B_2 \pm 1}{B_1} - 1 \right). \quad (6.6)$$

The two average horizontal fluid velocities will thus match, and through the Galilei transformation can be set to zero, either at $x \rightarrow \infty$ or $x \rightarrow -\infty$.

The most general form of solution parameter relationships, for which the exact solutions of the two-fluid model based on the formula (5.5) satisfy the PDE system (2.9) and the zero velocity shear condition at one of the infinities, is obtained through the substitution of the formulas (2.18), (2.19), (3.3), (3.4), and (6.6) into the equations (2.9). For example, for no velocity shear case at positive infinity, the following statement holds.

Proposition 6.1. *The two-fluid model (2.9) admits exact solutions corresponding to the dimensionless interface elevation formula (5.5) and satisfying the boundary condition $|v_1 - v_2| \rightarrow 0$ as $x \rightarrow \infty$ for the solution parameters $B_1, B_2, C_1, C_2, \gamma$ satisfying the relationships listed in Appendix C.*

In the relationships, the wave speed \hat{c} , is arbitrary as usual, due to the Galilei invariance of the model.

As an example, in Figure 13, we present a flood diagram corresponding to the exact solution (5.5) with parameters (C.1), (C.2) (first sign choices) for the following choice of the physical parameters:

$$\hat{c} = 1, \quad R = 3, \quad H = 1 \text{ m}, \quad g = 9.8 \text{ m/s}^2, \quad x_0 = t = 0, \quad S = 0.6. \quad (6.7)$$

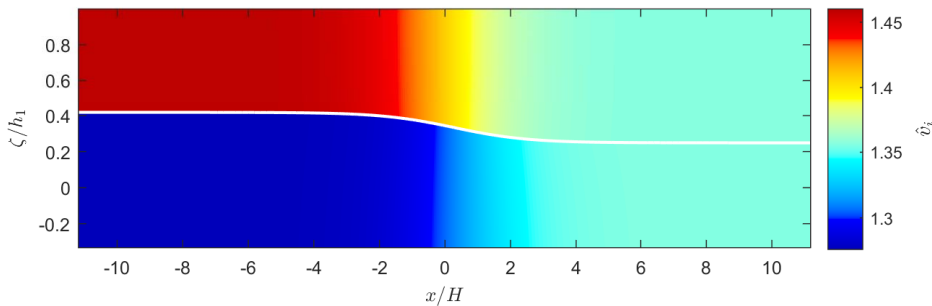


Figure 13: A flood diagram for a sample kink solution (5.5) satisfying $|v_1 - v_2| \rightarrow 0$ as $x \rightarrow \infty$. The diagram shows the dimensionless values of the fluid interface displacement (white curve), and the (x, z) -dependent horizontal velocities u_i computed through the formulas (2.13).

7 Conclusions and Discussion

The two-fluid model (2.9) is a nonlinear (1+1)-dimensional asymptotic approximation of the (2+1)-dimensional system of Euler equations and the interfacial conditions between two incompressible stratified fluids of different depth and density in a horizontal channel; the asymptotic assumption is the smallness of the fluid depth/characteristic length ratio. Mathematically, the model is given by a system of four nonlinear partial differential equations for the unknown fluid interface displacement, two layer-average horizontal velocities, and pressure. The PDE system involves mixed space-time third-order derivatives; it is not a ‘normal’ system of equations in the sense of [20].

The two-fluid model (2.9) depends on five physical constitutive parameters (2.17). In Section 2.3, a new dimensionless form (2.22) of the model was derived, involving a single dimensionless density ratio parameter (2.20). Due to the complexity of the nonlinear model, closed-form solutions of generic initial-boundary value problems for the system (2.9) or (2.22) are not available.

The original two-fluid system and its dimensionless version (2.22) admit space- and time-translation symmetries, allowing for a travelling wave solution ansatz, which was considered in Section 3. With the help of systematically calculated integrating factors, the four PDEs in this ansatz were reduced to an unusual single first-order nonlinear dimensionless ODE (3.8) with a rational polynomial right-hand side. The ODE (3.8) describes bidirectional travelling wave profiles of the fluid interface displacement; the layer-averaged velocities are consequently computed through the formulas (3.11), and the pressure is found from (3.4). Neither the ODE class (3.8) nor its equivalent form (3.13) have been extensively studied in literature. The implicit general solution can be clearly written through an integral, as well as possibly a combination of elliptic functions (Section 3.2), yet no formula for an explicit general solution is known to date.

In the current work, families of exact physically relevant traveling wave solutions of the two-fluid model were presented, arising from special solutions of the ODE (3.8). These multi-parameter families hold for wide ranges of physical fluid and channel parameters; they include the elevation and depression solitary waves, kink/anti-kink, and periodic traveling waves. Given by closed-form explicit expressions, the exact solutions elucidate some essential features of the model.

In Section 4, a family of cnoidal wave-type solutions (4.1), depending on eight constant parameters, was derived. The arbitrary parameters are the frequency parameter k , the wave amplitude and displacement B_1, B_2 , the traveling wave speed \hat{c} , the channel/fluid constants $S = \rho_1/\rho_2, h_1, h_2$, and the free fall acceleration g . The family contains periodic solutions of an arbitrary wavelength, as well as solitary wave-type solutions (4.10) corresponding to the infinite wavelength limit. In particular, both depression and elevation waves arise, for wide ranges of fluid density ratios S and channel depth parameters. All solutions are given by explicit formulae. The wavelength (4.8) of the periodic cnoidal solutions depends on the wave shape parameters k, B_1, B_2 . For the solitary wave solution, the wavelength is a function of the amplitude, and is determined by the expression (4.14); the amplitude exponentially decreases at infinity, matching the behaviour of solitary wave solutions of [1]. For all exact solutions of Section 4, one of the layer-average fluid velocities (v_1 for elevation waves, and v_2 for depression waves) has a constant value.

A different family of exact closed-form periodic solutions of the two-fluid model (2.9), also given by explicit expressions involving elliptic integrals, follows from solutions (5.1) to the ODE (3.8) (Section 5, Theorem 5.1). The exact solutions involve seven free constant parameters. The solution family includes examples of periodic solutions where neither of the layer-average fluid velocities vanishes. In the infinite wavelength limit, this solution family yields exact kink/anti-kink (front-type) solutions involving a hyperbolic tangent.

The exact explicit solutions found in the current contribution are given by relatively simple expressions involving well-studied elliptic integrals. The correctness of the solutions was verified explicitly by substitutions into the full two-fluid PDE system (2.9). Both solution families describe left- and right-propagating waves, depending on the choice of the sign of the wave speed \hat{c} . Additionally, there is a freedom in both families corresponding to independent choice of the sign in velocity formulas (3.11). Our solutions generally compare well with semi-numerical

ones presented in [1, 17].

Exact closed-form solutions considered in the current contribution were derived for $x \in (-\infty, \infty)$ without the consideration of boundary condition, under only natural physical limitations, in particular, the stable stratification assumption $0 < S < 1$, physical bounds $-h_2 < \zeta < h_1$ of the fluid interface displacement, and boundedness of pressure and average horizontal velocities. In particular, for the solitary wave-type and kink/anti-kink-type solutions obtained above, an intrinsic feature is the presence of velocity shear at $x \rightarrow \pm\infty$, as discussed in Section 6. On the contrary, in the literature analyzing solitary traveling waves, it is common to consider waves with no velocity shear, both for the two-fluid system and related models, such as general Green-Naghdi systems [1, 23]. For such setup, an important role is played by the critical depth ratio (6.3); in particular, for the fully nonlinear two-fluid equations (2.9), the solitary waves computed in [1] were reported to not exist when the depth ratio is critical, and to correspond to waves of elevation and depression for supercritical and subcritical depth ratios, respectively.

The above restrictions do not apply for the exact solutions derived in the current paper. In Section 6, it was shown that the presented exact solitary wave solutions do not satisfy the no velocity shear condition for any parameter choice, and thus complement the set of solutions previously studied in the literature. For the presented solutions, the critical depth ratio does not play a significant role. In particular, for the solitary waves, the fluid interface elevation (4.10) is independent of the depth ratio; both depression- and elevation-type solitons exist for wide ranges of amplitude, frequency, and channel/fluid parameters. Consequently, our solitary wave-type formulas do not apply for the amplitude-wavelength analysis (cf. [1], Figure 5). On the other hand, exact kink/anti-kink solutions presented in the current work can be chosen to have a velocity shear nonzero at one infinite boundary but zero at the other (Section 6.2).

An interesting feature of the traveling wave solutions of Section 4 is the identically constant value of the layer-average velocity of one of the fluids. It is of interest to compare this finding with experimental data, which would require new experiments, in particular, ones with nonzero velocity shear far from the solitary wave. Even for the zero velocity shear boundary condition case, the behaviour of layer-average velocities of solitary wave solutions were discussed neither in the work [1, 17] nor in the experimental paper [28].

Exact closed-form solutions of a complicated nonlinear PDE model, presented in the current work, form rich families involving free parameters and arbitrary physical constants; the solutions are given by rather simple formulas, having a clear physical meaning. Due to their simplicity, the solutions are expected to play the role of a natural testbed for various aspects of analysis of the current and related two-fluid models, numerical code testing, and various extensions.

Future work directions and open questions include the stability study of the presented solutions, in particular, in the view of the Kelvin-Helmholtz instability discussed in [11], and the possibility of the extension of the results of this work to regularized two-fluid models (e.g., [11]), including ones featuring nonzero surface tension [15] (see also [14]). Another work direction that is planned to be published in a follow-up paper is a systematic derivation of local conservation laws and symmetries of the two-fluid equations, and the comparison of the analytical properties of the two-fluid model with those of the classical Green-Naghdi-type models, the usual Euler equations, and other related models (cf. [27, 31, 32]).

It is of interest to study the possibility of derivation of other forms of exact solutions of

the nonlinear ODE (3.8), in particular, through the application of a semi-algorithmic simplest equation method [33]; a related important question is the possibility of existence of multi-soliton solutions for various two-fluid models.

Acknowledgements

The author is grateful to NSERC of Canada for the financial support of research through a Discovery grant.

References

- [1] W. Choi and R. Camassa, “Fully nonlinear internal waves in a two-fluid system,” *Journal of Fluid Mechanics*, vol. 396, pp. 1–36, 1999.
- [2] G. B. Whitham, *Linear and Nonlinear Waves*. John Wiley & Sons, 1974.
- [3] R. S. Johnson, “Camassa–Holm, Korteweg–de Vries and related models for water waves,” *Journal of Fluid Mechanics*, vol. 455, pp. 63–82, 2002.
- [4] R. Beals, D. H. Sattinger, and J. Szmigielski, “Multipeakons and the classical moment problem,” *Advances in Mathematics*, vol. 154, no. 2, pp. 229–257, 2000.
- [5] E. Pelinovsky, A. Slunyaev, O. Polukhina, and T. Talipova, “Internal solitary waves,” *Solitary Waves in Fluids*, ed. R. Grimshaw.
- [6] M. Miyata, “An internal solitary wave of large amplitude,” *La Mer*, vol. 23, no. 2, pp. 43–48, 1985.
- [7] Z. L. Mal'tseva, “Unsteady long waves in a two-layer fluid,” *Dinamika Sploshn. Sredy*, vol. 193, pp. 96–110, 1989.
- [8] W. Choi and R. Camassa, “Weakly nonlinear internal waves in a two-fluid system,” *Journal of Fluid Mechanics*, vol. 313, pp. 83–103, 1996.
- [9] A. Green, N. Laws, and P. Naghdi, “On the theory of water waves,” *Proceedings of the Royal Society of London A: Mathematical, Physical and Engineering Sciences*, vol. 338, no. 1612, pp. 43–55, 1974.
- [10] A. E. Green and P. M. Naghdi, “A derivation of equations for wave propagation in water of variable depth,” *Journal of Fluid Mechanics*, vol. 78, no. 02, pp. 237–246, 1976.
- [11] W. Choi, R. Barros, and T.-C. Jo, “A regularized model for strongly nonlinear internal solitary waves,” *Journal of Fluid Mechanics*, vol. 629, pp. 73–85, 2009.
- [12] W. Choi, “Modeling of strongly nonlinear internal gravity waves,” tech. rep., Los Alamos National Laboratory (LANL), Los Alamos, NM, 2000.
- [13] T.-C. Jo and W. Choi, “Dynamics of strongly nonlinear internal solitary waves in shallow water,” *Studies in Applied Mathematics*, vol. 109, no. 3, pp. 205–227, 2002.
- [14] V. Duchêne, S. Israwi, and R. Talhouk, “A new class of two-layer Green–Naghdi systems with improved frequency dispersion,” *Studies in Applied Mathematics*, 2016.
- [15] D. Lannes, “A stability criterion for two-fluid interfaces and applications,” *Archive for Rational Mechanics and Analysis*, vol. 208, no. 2, pp. 481–567, 2013.
- [16] G. El, R. H. Grimshaw, and N. F. Smyth, “Unsteady undular bores in fully nonlinear shallow-water theory,” *Physics of Fluids (1994-present)*, vol. 18, no. 2, p. 027104, 2006.

- [17] R. Camassa, P.-O. Rus as, A. Saxena, and R. Tiron, “Fully nonlinear periodic internal waves in a two-fluid system of finite depth,” *Journal of Fluid Mechanics*, vol. 652, pp. 259–298, 2010.
- [18] A. F. Cheviakov, “GeM software package for computation of symmetries and conservation laws of differential equations,” *Computer physics communications*, vol. 176, no. 1, pp. 48–61, 2007.
- [19] A. F. Cheviakov, “Computation of fluxes of conservation laws,” *Journal of Engineering Mathematics*, vol. 66, no. 1-3, pp. 153–173, 2010.
- [20] P. J. Olver, *Applications of Lie Groups to Differential Equations*, vol. 107. Springer Verlag, 2000.
- [21] G. W. Bluman, A. F. Cheviakov, and S. C. Anco, *Applications of Symmetry Methods to Partial Differential Equations*. Springer, 2010.
- [22] C. Su and C. Gardner, “Korteweg-de Vries equation and generalizations. III. Derivation of the Korteweg-de Vries equation and Burgers equation,” *Journal of Mathematical Physics*, vol. 10, no. 3, pp. 536–539, 1969.
- [23] V. Duch ene, S. Israwi, and R. Talhouk, “Shallow water asymptotic models for the propagation of internal waves,” *arXiv preprint arXiv:1306.1000*, 2013.
- [24] L. V. Ovsiannikov, *Group Analysis of Differential Equations*. Academic Press, 2014.
- [25] C. Kallendorf, A. F. Cheviakov, M. Oberlack, and Y. Wang, “Conservation laws of surfactant transport equations,” *Physics of Fluids*, vol. 24, no. 10, p. 102105, 2012.
- [26] O. Kelbin, A. F. Cheviakov, and M. Oberlack, “New conservation laws of helically symmetric, plane and rotationally symmetric viscous and inviscid flows,” *Journal of Fluid Mechanics*, vol. 721, pp. 340–366, 2013.
- [27] A. F. Cheviakov and M. Oberlack, “Generalized Ertel’s theorem and infinite hierarchies of conserved quantities for three-dimensional time-dependent euler and navier–stokes equations,” *Journal of Fluid Mechanics*, vol. 760, pp. 368–386, 2014.
- [28] C. G. Koop and G. Butler, “An investigation of internal solitary waves in a two-fluid system,” *Journal of Fluid Mechanics*, vol. 112, pp. 225–251, 1981.
- [29] K. Gorshkov, L. Ostrovsky, and I. Soustova, “Dynamics of strongly nonlinear kinks and solitons in a two-layer fluid,” *Studies in Applied Mathematics*, vol. 126, no. 1, pp. 49–73, 2011.
- [30] M. Przedborski and S. C. Anco, “Solitary waves and conservation laws for highly nonlinear wave equations modeling granular chains,” *arXiv preprint arXiv:1507.04759*, 2015.
- [31] Y. Matsuno, “Hamiltonian formulation of the extended Green–Naghdi equations,” *Physica D: Non-linear Phenomena*, vol. 301, pp. 1–7, 2015.
- [32] Y. A. Li, “Hamiltonian structure and linear stability of solitary waves of the Green-Naghdi equations,” *Journal of Nonlinear Mathematical Physics*, vol. 9, no. sup1, pp. 99–105, 2002.
- [33] N. A. Kudryashov, “Simplest equation method to look for exact solutions of nonlinear differential equations,” *Chaos, Solitons & Fractals*, vol. 24, no. 5, pp. 1217–1231, 2005.

A Coefficient Formulas for Theorem 4.1

The formula (4.1) provides a solution of the ODE (3.8) with (3.9) when the ODE and solution parameters are expressed in terms of B_1 , B_2 , k , S though the formulas

$$\alpha_0 = -\alpha_1 = \frac{A_4 B_2}{3k^2} (B_1 + B_2)(B_1 + B_2 k^2),$$

$$\gamma^2 = \frac{A_4 B_1}{4k^2 \alpha_1},$$
(A.1)

or through the formulas

$$\begin{aligned}\alpha_0 &= 0, & \alpha_1 &= -\frac{A_4}{3k^2}(B_2 - 1)(B_1 + B_2 - 1)(B_1 + k^2(B_2 - 1)), \\ \gamma^2 &= \frac{A_4 B_1}{4k^2 \alpha_1}.\end{aligned}\tag{A.2}$$

In (A.1), (A.2), the constants A_4 and A_1 are determined by (3.9) and (3.10), respectively.

B Coefficient Formulas for Theorem 5.1

The formula (5.1) yields a solution of the ODE (3.8) when the solution and the equation parameters γ , k , $\alpha_{0,1}$ are given in terms of the arbitrary constants B_1, B_2, S by

$$\begin{aligned}\alpha_0 &= -\alpha_1 = -\frac{A_4 B_1^3}{6B_2(1 - B_2^2)}, \\ \gamma^2 &= \frac{3B_2^2}{B_1^2}, & k^2 &= \frac{(1 - (B_1 - B_2)^2)}{B_2(2B_1 - B_2)(B_1^2 + (B_1 - B_2)^2) + (B_1 - B_2)^2},\end{aligned}\tag{B.1}$$

or through the formulas

$$\begin{aligned}\alpha_0 &= 0, & \alpha_1 &= \frac{A_4(2B_2 - B_1)(1 - (B_1 - B_2)^2)}{6B_2(1 - B_2^2)}, \\ \gamma^2 &= \frac{3B_1 B_2^2}{(2B_2 - B_1)(1 - (B_1 - B_2)^2)}, & k^2 &= B_2^{-2},\end{aligned}\tag{B.2}$$

or through the formulas

$$\begin{aligned}\alpha_0 &= \frac{A_4 B_1^3}{3(1 - B_2^2)} \frac{1 - (B_1 - B_2)^2}{B_2(4B_1^2 - 5B_1 B_2 + 2B_2^2) - 2B_2 + B_1}, & \alpha_1 &= 0, \\ \gamma^2 &= \frac{3}{B_1^2} \frac{B_2(2B_1 - B_2)(B_1^2 + (B_1 - B_2)^2) + (B_1 - B_2)^2}{1 - (B_1 - B_2)^2}, & k^2 &= \gamma^{-2}.\end{aligned}\tag{B.3}$$

In the expressions above, A_4 and A_1 are respectively determined by (3.9) and (3.10). Expressions for the constants A_2 and A_3 are straightforward to obtain; they are not listed here due to their complicated form and the lack of utility for writing down the physical solution components of the CC equations (2.9).

C Coefficient Formulas for Proposition 6.1

The relationship of the kink-anti-kink solution parameters for the case of no velocity shear at $x \rightarrow +\infty$ is given in terms of the arbitrary constant S , for any value of the wave speed \hat{c} , by

$$C_2 = C_1 \left(\frac{B_2 + 1}{B_1} - 1 \right),\tag{C.1}$$

and the formulas

$$B_1 = \mp \frac{2\sqrt{S}}{1-S}, \quad B_2 = -\frac{1 \pm \sqrt{S}}{1 \mp \sqrt{S}}, \quad \gamma^2 = \frac{3(1-S)^2}{4S}, \quad C_1^2 = \frac{1 \mp \sqrt{S}}{(1 \pm \sqrt{S})^3}, \quad (\text{C.2})$$

or through the formulas

$$B_1 = \pm \frac{2\sqrt{S}}{1+S}, \quad B_2 = \frac{-1+S \pm 2\sqrt{S}}{1+\sqrt{S}}, \quad \gamma^2 = \frac{3(1+S)^2}{4S}, \quad C_1^2 = \frac{1}{1-S}. \quad (\text{C.3})$$

The plus or minus signs can be chosen independently.